Polypropylene/Montmorillonite Composites and Their Application in Hybrid Fiber Preparation by Melt-Spinning

Xiuqin Zhang,[1] Mingshu Yang,[2] Ying Zhao,[2] Shimin Zhang,[2] Xia Dong,[1] Xuexin Liu,[1] Dujin Wang,[1] Duanfu Xu[1]

[1]*State Key Laboratory of Polymer Physics and Chemistry, Joint Laboratory of Polymer Science and Materials, Center for Molecular Science, Institute of Chemistry, Chinese Academy of Sciences, Beijing 100080, China*
[2]*State Key Laboratory of Engineering Plastics, Joint Laboratory of Polymer Science and Materials, Institute of Chemistry, Chinese Academy of Sciences, Beijing 100080, China*

Received 31 July 2003; accepted 9 November 2003

ABSTRACT: Polypropylene (PP)/organomontmorillonite (OMMT) nanocomposites have been successfully prepared by melt intercalation by using the conventional method of twin-screw extrusion and subsequently submitted for melt-spinning. The structure and properties of the PP/clay nanocomposites and hybrid fibers were characterized by scanning electron microscopy (SEM), transmission electron microscopy (TEM), X-ray diffraction (XRD), differential scanning calorimetry (DSC), and crystallization dynamics, etc. The organoclay layers were found to disperse in the PP resin at the nanometer level. The nanoscaled OMMT layers, dispersed in the PP matrix, actually played the role of heterogeneous nuclei species in the process of PP crystallization and increased the nucleation speed of the composites, hereby leading to the increase of crystallization rate of the as-spun fiber. Meanwhile, it was found that the crystallinity of PP/OMMT hybrid fibers is much higher than that of pure PP fiber at the same draw ratios, whereas the orientation of PP/OMMT hybrid fibers is much lower than that of pure PP fiber at the same draw ratios. Because of the effective intercalation of OMMT into PP matrix, the nanocomposites have good spinnability, and the moisture absorption of the final PP fiber is improved.© 2004 Wiley Periodicals, Inc. J Appl Polym Sci 92: 552–558, 2004

Key words: polypropylene/organomontmorillonite nanocomposite; crystallization; fibers

INTRODUCTION

In the last two decades, research on polymer/clay nanocomposites has been extensively reported[1–5] because of their superior physical and mechanical behaviors over their more conventional microcomposite counterparts. One promising strategy for preparing polymer/clay nanocomposites is the intercalation of monomers or polymers into layered silicate hosts. Polymer intercalation techniques mainly include melt-intercalation and solution polymerization intercalation. Compared with *in situ* intercalative polymerization, polymer melt-direct intercalation does not need compatible solvents, accordingly simplifying the after-treating process, so the melt intercalation method gradually becomes the mainstream for the preparation of the intercalated polymer nanocomposites.[6] This methodology is especially effective technology in the case of polyolefin-based nanocomposites.[7–8]

Much research has been reported on preparation and characterization of polypropylene (PP)/clay nanocomposites, focusing on the dispersed morphology of the clay particles,[9] their excellent properties,[10–12] and their rheological behavior,[13] etc. Further investigation on the application of the above-mentioned PP/clay nanocomposites, as far as we know, has seldom been reported. In this article, we prepared melt-intercalation nanocomposites of PP/organomontmorillonite (PP/OMMT) and studied the melt-spinning process and tried to elucidate the relationship between the nanocomposites structure and the PP hybrid fiber properties.

EXPERIMENTAL

Materials

PP with a melt flow index (MFI) of 44 g/10 min was prepared by means of chemical degradation.[14] Na^+-based montmorillonite with a cation-exchange capacity value of 90–100 mmol/100 g and organomontmorillonite were prepared in our institute.[15] Polypropylene grafted with maleic anhydride (PP-*g*-MAH) was purchased from the Tianjin Institute of Chemical

Correspondence to: D. Wang (djwang@iccas.ac.cn).
Contract grant sponsor: National Natural Science Foundation of China; contract grant number: 50290090.
Contract grant sponsor: Polymer Science and Materials Team Building Project.
Contract grant sponsor: Directional Project from CAS.

Journal of Applied Polymer Science, Vol. 92, 552–558 (2004)

Fiber (Tianjin, China). Linear polystyrene (PS) was provided by Beijing Yanshan Petrochemical Factory (Beijing, China).

Preparation of PP/OMMT nanocomposites

PP/OMMT nanocomposites were prepared via polymer melt-direct intercalation at 210°C by using a twin-screw extruder. The selected recipe for the nanocomposite is PP, 100 wt %; OMMT, 5 wt %; PP-*g*-MAH, 2 wt %; and PS, 1 wt %. PP-*g*-MAH was used as a compatibilizer to promote the interaction between PP molecules and OMMT layers.[16–17] The addition of PS can further destroy the dense structure of polypropylene, consequently endowing such PP fiber with excellent properties for fabric weaving.

Melt spinning process

Before being submitted for melt spinning, the PP and PP/OMMT nanocomposites were dried in a vacuum oven for 4 h at 80°C. Melt spinning was performed on a single-screw ($L/D = 25$) melt extruder with a spinneret containing 48 orifices, each 0.35 mm in diameter. The extruder was set with five different temperature zones of 200, 220, 230, 225, and 200°C at the feed, metering, melt-blending, die, and spinneret sections, respectively. The as-spun filaments were collected at a take-up speed of 500 m/min and drawn at 100°C on a four-positioned drawing platform.

Characterization of nanocomposites and fibers

Evaluation of dispersity of OMMT in PP matrix

The dispersibility of the silicate layers in the nanocomposites was evaluated by combination of XRD and TEM. XRD analysis between 1 and 10° was performed for the melt-processed film of PP/OMMT by using a Rigaku D-MAX-2500 X-ray diffractometer with CuKα radiation at a generator voltage of 45 kV and a generator current of 100 mA. The 100-nm ultrasectioned slice of PP/OMMT resin was investigated by a Hitachi H-800 TEM, with an acceleration voltage of 100 kV. Fibers for TEM measurement were embedded in a capsule with an embedding agent polymerized at 70°C for 48 h. The embedded sample was ultrathin-sectioned by using a microtome equipped with a glass knife. Transmission electron micrographs were obtained with a JEOL 100CX by using an acceleration voltage of 100 kV.

X-ray and infrared dichroism analysis of PP and PP/OMMT fibers

To measure the crystallinity and the grain size of PP and PP/OMMT hybrid fibers, XRD data between 6 and 36° were collected by using a Rigaku D/MAX-RB X-ray diffractometer with CuKα radiation at a generator voltage of 40 kV and a generator current of 50 mA. The fibers were crushed into fragments before measurement. Grain size was calculated from the Scherrer's equation: $L = 0.9\lambda/\beta \cos \theta$, where L is the crystallite dimension, λ is the wavelength of CuKα (1.54 Å), β is the peak breadth at half-maximum intensity, and θ is the Bragg angle.

The degree of fiber orientation was measured by polarization infrared spectroscopy method with a Bruker EQUINOX 55 spectrometer. The parallel and perpendicular spectra were collected by averaging 32 scans at a 4 cm^{-1} resolution.

Crystallization rate measurement

Crystallization rate was expressed by the variation of depolarized light intensity of the samples. The experiments were carried out on a crystallization recorder (DPL-II) built in our laboratory. The sample was first melted at 250°C for 40 s to eliminate the influence of crystallization history, followed by placing the sample into a crystallization oven at a given temperature. The light intensity curve was recorded at the following selected crystallization temperatures: 120, 110, 100, 80, and 60°C. The crystallization half-life-time of $t_{1/2}$ is the time period of the half-maximum intensity.

Thermal analysis

The crystallization behavior of PP/OMMT nanocomposites was investigated by means of DSC on a DSC822e (Mettler Toledo) with samples weights of 4–6 mg. All operations were performed under a nitrogen environment. The samples were heated to 200°C and held in the molten state for 2 min to eliminate the influence of thermal history and then cooled at a rate of 10°C/min to room temperature. Both endothermal flow and exothermal flow were recorded.

SEM measurements of PP fibers

The surface morphology of both pure PP fiber and PP/OMMT hybrid fiber was studied by using a JEOL JSM-35CF SEM with an acceleration voltage of 15 kV.

Tensile measurements of PP fibers

The tensile properties of fibers were measured in a tensile testing machine (YG001A) at a falling speed of 60 mm/min. At least 10 tests were averaged for each sample.

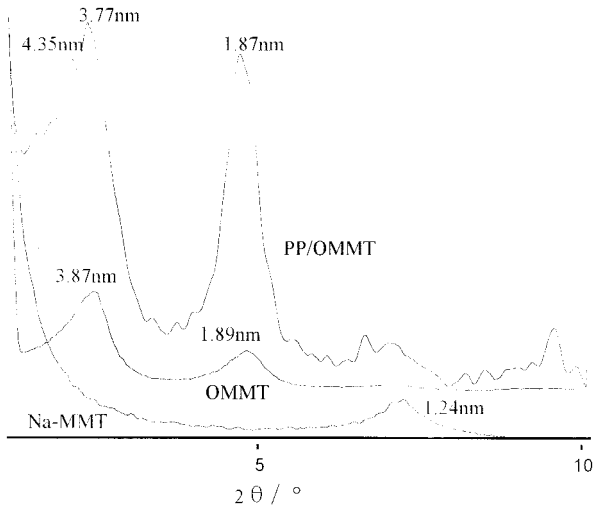

Figure 1 XRD curves of Na-MMT, OMMT, and PP/OMMT.

Moisture absorption measurements

The fibers were washed and dried in a vacuum oven for 3 h at 105°C. Then, the fibers were placed in a temperature-/humidity-equilibrated box for more than 5 h, in which the temperature was controlled at 20°C and the humidity was controlled at 65%. The moisture absorption was calculated from the following equation: moisture absorption (%) = $(W_1 - W_0)/W_0 \times 100\%$, where W_1 is the wet weight of the fiber, and W_0 is the dry weight of the fiber.

RESULTS AND DISCUSSION

Dispersibility of OMMT in PP/OMMT nanocomposite

The X-ray diffraction data in the range of $2\theta = 1$–10° of Na-MMT, OMMT, and PP/OMMT nanocomposites are shown in Figure 1.

The XRD pattern of Na-MMT contains a peak at $2\theta = 7.10°$, while two strong peaks at $2\theta = 2.28°$, 4.66° are observed for OMMT and three strong peaks at $2\theta = 2.03°$, 2.34°, 4.72° are observed for PP/OMMT. The interlayer spacing was calculated according to the Bragg equation to be 1.24 nm for Na-MMT, 3.87 and 1.89 nm for OMMT, and 4.35, 3.77, and 1.87 nm for PP/OMMT, respectively. The above XRD results indicate that organic treatment of MMT can expand or exfoliate the silicate layers. The slightly increased interlayer spacing after melt mixing is presumably due to additional intercalation of PP resin. The XRD results are in qualitative agreement with the results for other polypropylene hybrids.[13,16,17]

TABLE I
Crystallization Rate ($t_{1/2}$) of Pure PP and PP/OMMT Nanocomposites

T (°C)	60	80	100	110	120
PP ($t_{1/2}$)/s	10.6	14.0	28.03	44.84	201.2
PP/OMMT ($t_{1/2}$)/s	10.8	14.4	18.12	27.84	63.0

Figure 2 shows the TEM photographs of PP/OMMT nanocomposite and hybrid fiber. The silicate layers were found to disperse uniformly in the polymer matrix with average width/thickness of 20–50 nm. Similar dispersion results were also observed by Jayaraman et al.[8] and Okamoto et al.[9] The TEM images of PP/OMMT nanocomposites show that silicate layers were exfoliated or intercalated, which provided excellent spinnability of the PP/OMMT nanocomposites. Compared with PP/OMMT nanocomposite, the OMMT dispersion size increased slightly in PP/OMMT hybrid fiber, which implies that agglomeration may occur for the nanolayered silicate layers in the process of melt-spinning.

Crystallization analysis of pp/ommt nanocomposites

Table I shows the crystallization rate ($t_{1/2}$) of pure PP and PP/OMMT nanocomposite under several crystallization temperatures. The $t_{1/2}$ values prove that at higher temperature OMMT influences the crystallization rate of nanocomposites more effectively. Further-

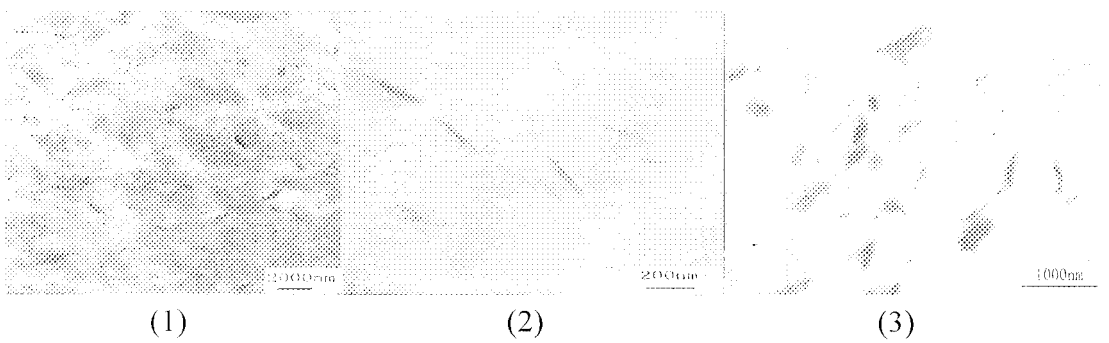

Figure 2 TEM images of PP/OMMT nanocomposite (1, 2) and hybrid fiber (3).

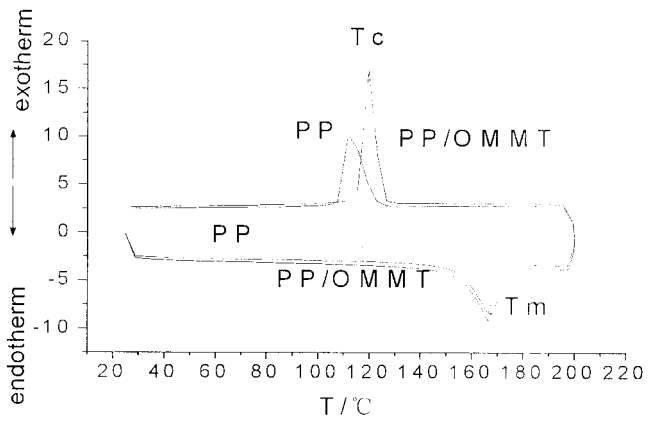

Figure 3 DSC curves of PP and PP/OMMT resins.

more, the crystallization rate of PP/OMMT is faster than that of pure PP at a higher temperature. Therefore, it can be concluded that the introduction of OMMT increased the crystallization rate of PP chains, especially at high temperature.[18]

The crystallization rate of polymer is decided by two main factors: the crystal growing rate and the nucleation rate. The nucleation modes include homogeneous nucleation and heterogeneous nucleation. Homogeneous nucleation starts spontaneously by chain aggregation below the melting point and requires some time. While thermal motion of molecules is drastic at high temperature, which makes nuclei unstable, homogeneous nucleation occurs easily at low temperature. Heterogeneous nucleation induced by additives forms instantly and is independent of time, so it can easily occur at high temperature.[19] On the other hand, the crystallization rate is decided by the crystal growing rate at low temperature and is controlled by the nucleation rate at high temperature. Therefore, when the OMMT layers were exfoliated or enlarged in the PP/OMMT nanocomposite, the number of the heterogeneous nuclei in PP/OMMT is much larger than that in pure PP, resulting in the crystallization rate of PP/OMMT at high temperature being much greater than that of pure PP. It was also found that the difference of the crystallization time between pure PP and PP/OMMT nanocomposite increases with increasing crystallization temperature. All these results indicate that the OMMT layers dispersed in PP matrix have a dramatic heterogeneous nucleation effect on the crystallization process.

Figure 3 presents the melting and crystallization curves of pure PP and PP/OMMT. As can be seen, the crystallization temperature of PP/OMMT is higher than that of pure PP, and the crystallization peak of PP/OMMT is sharper than that of pure PP. The melting point, however, is almost the same for both PP and PP/OMMT. This is to say, the presence of OMMT decreases the crystallization time markedly of the PP chains and increases the crystallization temperature of the PP matrix. This effect can be explained by the assumption that the silicate layers act as efficient heterogeneous nucleating agents for the crystallization of PP matrix. The results are consistent with those of PP/clay nanocomposites reported by other researchers.[4,12,18–20]

Spinnability of PP/OMMT hybrid resins into fibers

Typical spinning conditions used have been mentioned in Experimental. Due to the good dispersity of OMMT in PP matrix, we were able to successfully make as-spun fibers from PP/OMMT nanocomposites and did not need to adjust the spinning conditions as used for pure PP resins. After drawing 2–4 times, fiber fineness was achieved in the range of 0.7–6 dtex: tenacity was in the range of 1.5–6 g/den and elongation was in the range of 15–200%. These values demonstrate the practical applicability of the hybrid PP fibers. Fibers with specific performances have different uses. For example, when fiber is used for clothing, the lower strength is beneficial to antipilling of clothing.

X-ray and infrared dichroism analysis PP/OMMT hybrid fiber

Isotactic polypropylene is a multicrystalline polymer and generally has five crystalline forms (i.e., α, β, γ, δ, and pseudohexagonal). The XRD study shows that the addition of OMMT greatly affects the crystalline form of as-spun fibers (Fig. 4). It was found from the XRD curves that pure PP as-spun fiber and PP/OMMT as-spun fiber exhibit different crystalline diffraction peaks. XRD spectra of pure PP as-spun fiber showed distinct pseudohexagonal crystalline diffraction peaks at $2\theta = 15.2°$ and 21.4°, whereas PP/OMMT as-spun fiber exhibits distinct α-crystalline diffraction peaks at

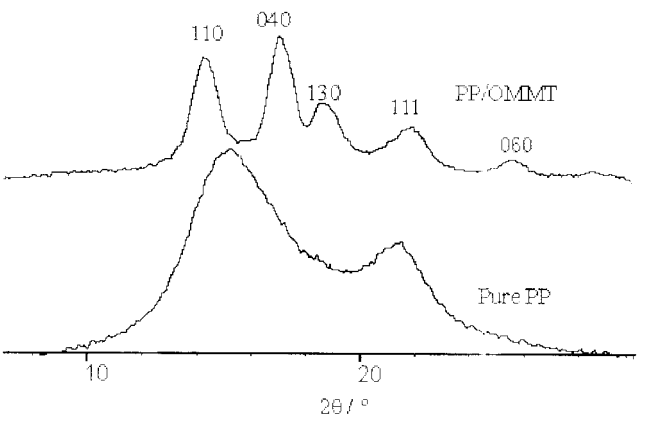

Figure 4 XRD curves of as-spun fibers.

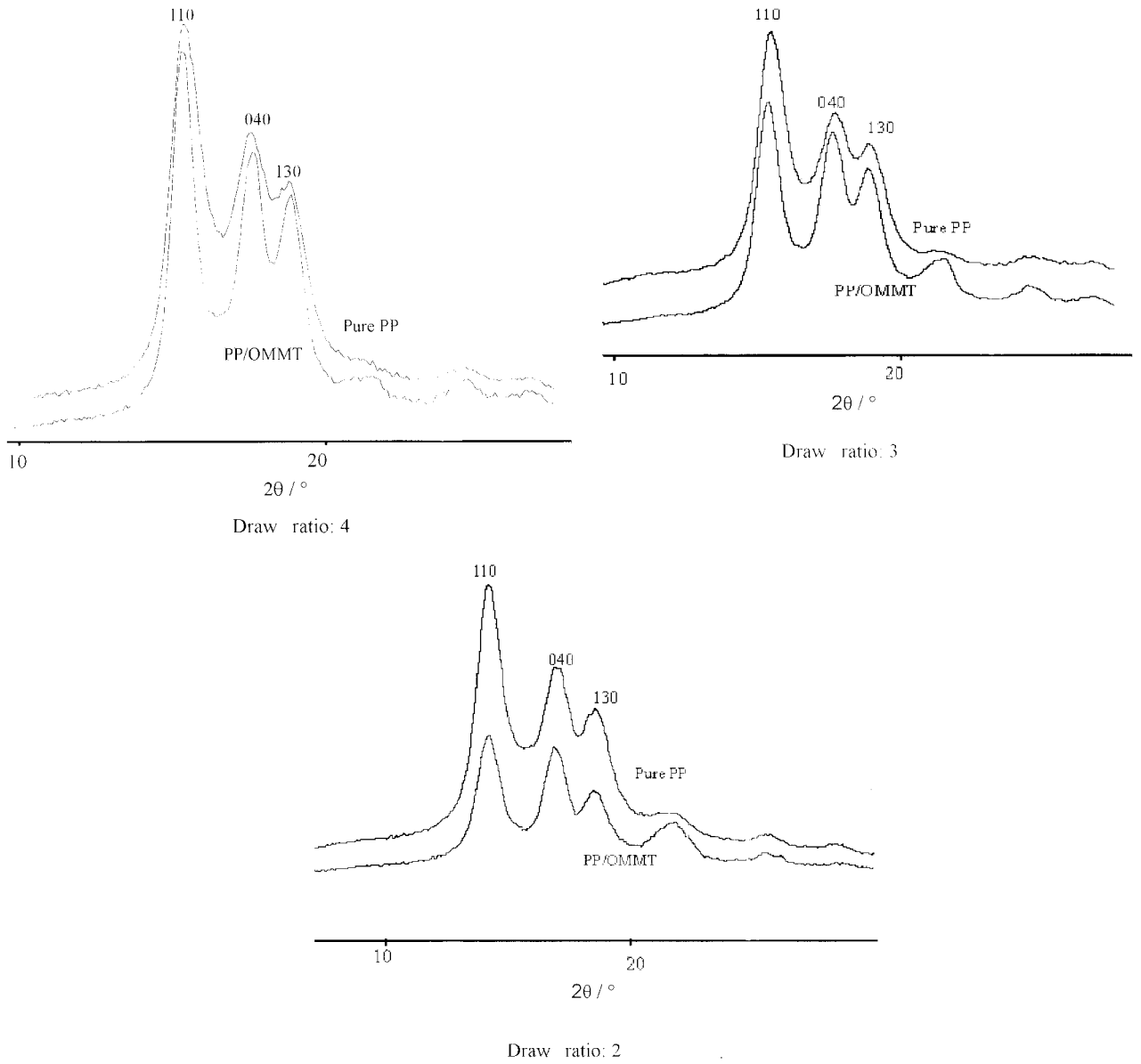

Figure 5 XRD curves of pure PP-drawn fiber and PP/OMMT hybrid-drawn fiber.

2θ = 14.26°, 17.05°, 18.70°, 21.76°, and 25.59°, which often appear under more efficient crystallization conditions, such as drawing and annealing, etc. The XRD results implied that the crystallization rate of PP/OMMT as-spun fiber is much faster than that of pure as-spun PP fiber, in good agreement with the results of PP/OMMT nanocomposites. As the stable α-crystalline form of PP/OMMT as-spun fiber is easily obtained, it is possible for us to prepare polypropylene fully drawn yarn (FDY) by one-step spinning technique.

It was found that the α-crystalline form dominates for all the drawn fibers (Fig. 5), meaning that the addition of OMMT does not affect the crystal form of the final PP molecules. Compared with the XRD curves of pure PP fiber, the relative intensity of the diffraction peaks (040, 130, 111, 060) for PP/OMMT hybrid fibers increased, taking the (110) peak as reference. A possible reason is that the addition of OMMT promotes the nucleation and growth of PP crystals in an essential way and perfects the α-crystalline form. It

TABLE II
Crystallinity and Orientation of Drawn Fibers

Sample	Crystallinity (%)	Orientation (%)
Pure PP (draw ratio: 4)	43.7	82.4
PP/OMMT (draw ratio: 4)	66.0	50.0
Pure PP (draw ratio: 3)	58.2	55.9
PP/OMMT (draw ratio: 3)	73.8	35.0
Pure PP (draw ratio: 2)	51.0	45.3
PP/OMMT (draw ratio: 2)	67.0	32.7

TABLE III
Crystallite Size and 2θ Values of (110) Plane of Pure PP Fiber and PP/OMMT Hybrid Fiber

Sample	2θ (°)	Crystallite size (Å)
Pure PP (draw ratio: 4)	14.23	60.27
PP/OMMT (draw ratio: 4)	14.15	75.44
Pure PP (draw ratio: 3)	14.29	63.05
PP/OMMT (draw ratio: 3)	14.15	69.76
Pure PP (draw ratio: 2)	14.17	71.70
PP/OMMT (draw ratio: 2)	14.14	74.06

was also found from Figure 5 that the integral area of the amorphous domains decreases with the addition of OMMT into the PP matrix, indicating that the crystallinity of PP/OMMT hybrid fiber was improved.

The crystallinity and orientation of the PP/OMMT drawn fibers were calculated by curve fitting of the XRD graphs and polarized infrared spectroscopy, respectively (Table II). The results show that the crystallinity of fibers at lower draw ratios (2–3) increases with draw ratios, but decreases as the draw ratio is larger than 3, because the restriction on the stretched chains becomes greater and thus makes the chains more difficult to reconfigure into the correct helical registration that is necessary for crystallization.[21] In addition, the crystallinity of PP/OMMT hybrid fibers is much higher than that of pure PP fiber at all draw ratios. This may be attributed to the high surface energy of the nanoscaled OMMT layers, which is beneficial to crystal growth and crystal stability.

The orientation of both PP and PP/OMMT fibers increased with increasing draw ratios. The orientation of PP/OMMT hybrid fibers is much lower than that of pure PP fiber at the same draw ratios, which is beneficial to moisture absorption and dying ability of PP/OMMT hybrid fibers.[22]

The grain sizes of the (110) plane of PP crystal for pure PP fiber and PP/OMMT hybrid fibers were obtained by Scherrer's equation (Table III). The 2θ values changed little for PP/OMMT hybrid fiber, compared with pure PP fiber, which means that the addition of OMMT did not alter the crystalline form. The grain size of plane (110) of PP in PP/OMMT hybrid fiber, however, is much larger than that of pure PP, indicating that the introduction of OMMT induced a variation in growing habit of the PP crystals.

Surface morphology and moisture absorption of PP/OMMT hybrid fibers

The SEM micrographs show that the surface of PP fiber is smooth, whereas that of PP/OMMT hybrid fiber has many flaws and grooves (Fig. 6), which may result in the major change of the physical properties, such as antielectricity and moisture absorption. The moisture absorption of fiber is determined by three factors: polar group content, flaws and grooves, and amorphous content. If the fiber presents more polar groups, more flaws and grooves, and more amorphous regions, the moisture absorption will increase, because water being polar interacts strongly with other polar groups. Flaws and grooves can provide channels for water molecules entering into the fiber, whereas amorphous regions are responsible for water penetration. The moisture absorptions of pure PP and PP/OMMT fiber are shown in Table IV. The moisture

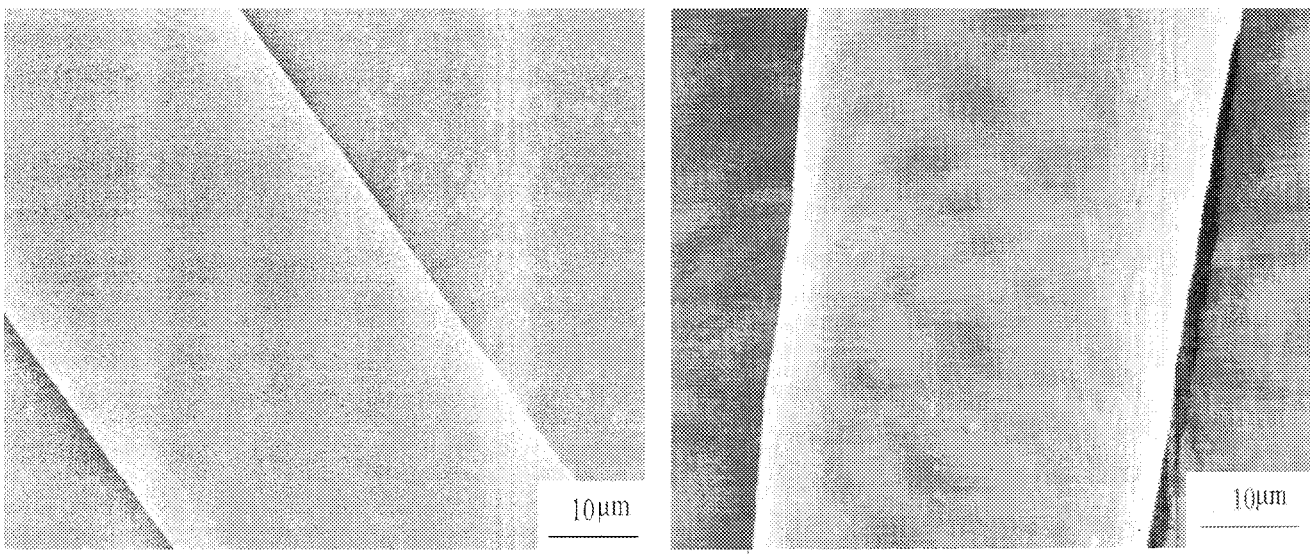

Figure 6 SEM images of pure PP fiber and PP/OMMT hybrid fiber.

TABLE IV
Moisture Absorption of Pure PP and PP/OMMT Fibers

Sample	Draw ratio	Moisture absorption (%)
Pure PP	4	0.40
PP/OMMT	4	0.55
Pure PP	3	0.45
PP/OMMT	3	0.60
Pure PP	2	0.50
PP/OMMT	2	0.63

absorption of PP/OMMT fiber is higher than that of pure PP fiber. The main reasons are that the introduction of OMMT and PP-*g*-MAH increased the amount of hydrophilic groups, and the addition of PS led to the formation of flaws and grooves on the fiber surface. All these factors aid the improvement of moisture absorption. On the other hand, the introduction of OMMT increases the crystallinity of hybrid fibers, thus decreasing the hydrophilic properties of the fibers. So, the improvement of the moisture absorption of PP/OMMT fiber is an equilibrating/competing result, and in the present experiment, the influence of the polarized group increase prevails over that of the crystallinity enhancement.

CONCLUSION

In conclusion, PP/OMMT nanocomposites have been successfully prepared by melt intercalation by using a conventional twin-screw extrusion technique and the modified resin was consequently made into fibers. The particles of silicate layers were found to disperse in the matrix resin at the nanometer level. The nanoscaled OMMT layers dispersed in the PP matrix actually played the role of heterogeneous nuclei species in the process of PP crystallization and increased the nucleation speed of the composites, thus leading to the increase of crystallization rate of the as-spun fiber. On the other hand, the crystallinity of PP/OMMT hybrid fibers is much higher than that of pure PP fiber at the same draw ratios, and the orientation of PP/OMMT hybrid fibers is much lower than that of pure PP fiber at the same draw ratios. It was also found that the surface of the PP/OMMT fiber has many flaws and grooves by which the moisture absorption of the PP/OMMT hybrid fiber was improved.

This work was supported by National Natural Science Foundation of China (NSFC, Grant No. 50290090), Polymer Science and Materials Team Building Project, and Directional Project from CAS.

References

1. Zeng, C. C.; Lee L. J. Macromolecules 2001, 34, 4098.
2. Kim, B. H.; Jung, J. H.; Hong, S. H.; Joo, J. Macromolecules 2002, 35, 1429.
3. Zhu, J.; Morgan, A. B.; Lamelas, F. J.; Wilkie, C. A. Chem Mater 2001, 13, 3774.
4. Liu, X. H.; Wu, Q. J. Polymer 2001, 42, 10013.
5. Chang, J. H.; Seo, B. S.; Hwang, D. H. Polymer 2002, 43, 2969.
6. Vaia, R. A.; Ishii, H.; Giannelis, E. P. Chem Mater 1993, 5, 1694.
7. Wang, K. H.; Choi, M. H.; Koo, C. M.; Choi, Y. S.; Chung, I. J. Polymer 2001, 42, 9819.
8. Marchant, D.; Jayaraman, K. Ind Eng Chem Res 2002, 41, 6402.
9. Nam, P. H.; Maiti, P.; Okamoto, M.; Kotaka, T.; Hasegawa, N.; Usuki, A. Polymer 2001, 42, 9633.
10. Kawasumi, M.; Hasegawa, N.; Kato, M.; Usuki, A.; Okada, A. Macromolecules 1997, 30, 6333.
11. Manias, E.; Touny, A.; Wu, L.; Strawhecker, K.; Lu, B.; Chung, T. C. Chem Mater 2001, 13, 3516.
12. Maiti, P.; Nam, P. H.; Okamoto, M. Macromolecules 2002, 35, 2042.
13. Solomon, M. J.; Almusallam, A. S.; Seefeldt, K. F.; Somwangthanaroj, A.; Varadan, P. Macromolecules 2001, 34, 1864.
14. Marisa, C. G. R.; Fernanda, M. B. C.; Stephen, T. B. Polym Test 1995, 14, 369.
15. Qi, Z. N.; Wang, S. J.; Zhou, W. Y. China Pat. CN1247206A. (1998).
16. Hasegawa, N.; Kawasumi, M.; Kato, M.; Usuki, A.; Okada, A. J Appl Polym Sci 1998, 67, 87.
17. Kim, K.-N.; Kim, H.; Lee, J.-W. Polym Eng Sci 2001, 41, 1963.
18. Xu, W. B.; Ge, M. L.; He, P. S. J Polym Sci, Part B: Polym Phys 2002, 40, 408.
19. Ma, D. Z. Structure and Performance of Polymer; Science Press: Beijing, 2000.
20. Ma, J. S.; Zhang, S. M.; Qi, Z. N.; Li, G.; Hu, Y. L. J Appl Polym Sci 2002, 83, 1978.
21. Ran, S. F.; Zong, X. H.; Fang, D. F.; Hsiao, B. S.; Chu, B. J. Macromolecules 2001, 34, 2569.
22. Yu, C. B.; Zhu, M. F.; Shong, X. Y.; Chen, Y. M. J Appl Polym Sci 2001, 82, 3172.